Chapter 21

Ionic Liquids Applied to Improve the Dispersion of Solids in Elastomers

Magdalena Maciejewska and Marian Zaborski

Additional information is available at the end of the chapter

http://dx.doi.org/10.5772/58980

1. Introduction

Rubber compounds consist of an elastomer matrix and solid additives. The most important role of these additives is to act as fillers and vulcanization activators in the case of sulfur crosslinked elastomers. Elastomers are filled with small and hard particles to improve their mechanical properties, such as resistance to abrasion, elastic modulus, and hardness [1]. Reinforcing fillers added to an elastomer can provide a rubber product with a very high tensile strength or tear resistance [2]. The basic requirement to achieve the optimum reinforcement is a fine and homogeneous dispersion of filler particles in the elastomer matrix, which results in effective interactions and good adhesion at the elastomer/filler interface. Due to their unique physical and chemical properties, over the past few years polymer composites with nanofillers such as nanosilica, carbon black, layered silicates, and carbon nanotubes have been widely discussed [3, 4]. It has been proven that the degree of dispersion of nanofiller particles is crucial to achieve the ultimate required properties of nanocomposites [5]. Unfortunately, nanofillers exhibit a high tendency to agglomerate in the elastomer matrix because of their high surface energy [6, 7]. Therefore, it is technologically challenging to obtain a homogeneous dispersion of filler nanoparticles in elastomers.

Recently, ionic liquids (ILs) have been widely used to improve the degree of dispersion of nanoparticles in polymers, particularly in elastomers [8-10]. ILs are typically organic salts with the melting points below 100 °C [11]. Due to their unique properties such as thermal, chemical, and electrochemical stability, low vapor pressure, and high ionic conductivity, ILs have attracted much attention for applications in polymer science [11-13], particularly toward developing conducting polymer composites. ILs have excellent ionic conductivity up to their decomposition temperature, which enables them to play an important role in electrolyte matrices. For example, N-ethylmethylimidazolium bis(trifluoromethanesulfonyl)imide

(EMITFSI) was used for the preparation of flexible solid polymer electrolytes based on acrylonitrile-butadiene elastomers and poly(ethylene oxide) [14]. The formation of either cationic and anionic interpenetrating or semi-interpenetrating polymer networks caused a considerable increase in the tensile strength and elasticity of the polymer electrolyte. When swollen in EMITFSI, the composites exhibited good mechanical properties and elongation at break, and an ionic conductivity higher than 10^{-4} S cm^{-1} at room temperature. Similar results were obtained for interpenetrating polymer networks containing alkylpyrrolidinium bis(trifluoromethanesulfonyl)imides [15]. Conductive NBR composites with an ionic conductivity of 2.54×10^{-4} S cm^{-1} have also been prepared using 1-butyl-3-methylimidazolium bis(trifluoromethylsulfonyl)imide [16]. This ionic liquid was also used to produce conductive composites from poly(methyl methacrylate) containing in situ formed silica [17]. When increasing the IL content, the conductivity of the obtained hybrid ionogels increased, and a decrease in the Young's modulus was observed as a result of the plasticizing effect of ILs. Similar results were reported for N-ethylimidazolium bis(trifluoromethylsulfonyl)imide (EITFSI). Composites consisting of NBR and ionic liquid were prepared as elastic and thermally stable polymer electrolytes, and EITFSI showed good miscibility with NBR. The presence of lithium salts in NBR/EITFSI composites enhanced the ionic conductivity approximately 100 times to reach 1.0×10^{-4} S cm^{-1} at 30 °C [18].

Moreover, some ILs have been suggested to be used for solubilizing metal oxides [19]. This property could be useful in the improvement of dispersion degree of metal oxide particles in elastomers. 1-allyl-3-methylimidazolium chloride (AMICl) was applied to improve the dispersion of particles in carbon black-filled elastomers. Attractive interactions between the carbon black surface and AMICl, which result from the interaction of π-electrons of graphitic structures at the carbon black surface with the cations of ionic liquid, have been demonstrated. AMICl acted as plasticizer at the carbon black surface and accelerated the formation of the carbon black network in the elastomer matrix, supporting the depletion of polymer chains from the space between carbon black aggregates. Moreover, an increase in the conductivity of elastomer composites was observed [10]. ILs have also been reported to improve the dispersion of silica and clays [20, 21]. For example, 1-methylimidazolium sorbate was used as modifier for silica to increase the interfacial interactions between the filler and styrene-butadiene rubber (SBR). As a result, the mechanical performance of SBR/silica composites were effectively improved, and similar results were also achieved for 1-methylimidazolium methacrylate (MimMa). The ionic liquid was reactive toward SBR through the graft copolymerization onto elastomer chains during vulcanization. Hydrogen bonding between silica particles and the ionic unit of MimMa was shown to be present. As a result, the interactions between silica particles were weakened, and the filler networking of silica in SBR was effectively restrained. An improvement in the dispersion of silica and the mechanical properties of vulcanizates, particularly damping behavior and abrasion resistance, was observed [8]. Imidazolium salts have been demonstrated as excellent cationic treatments for layered silicates (clays). The best activity was achieved when one of the imidazolium alkyl groups of the IL was a C16 aliphatic chain [22]. This IL exhibited excellent compatibility with polymers, and due to its high thermal stability, it enabled high-temperature curing and melt processing. Trihexyltetradecylphosphonium tetrafluoroborate was used for cationic exchange on the surfaces of natural and synthetic nanoclays [21]. Significant enhancements in the thermal stability of nanoclays were achieved, up to 150 °C, compared with conventional quaternary ammonium-modified silicates. These IL-modified nanoclays have been melt blended with poly(ethylene terephthalate) (PET), and optically transparent nanocomposites with high levels of exfoliation have been produced, in which nanoclay platelets were uniformly dispersed in the PET matrix.

Polymer composites filled with carbon nanotubes (CNTs) are of particular interest for the development of conductive polymer nanocomposites or nanoelectronic devices [23, 24]. A major problem in this field is to ensure the homogeneous dispersion of carbon nanotubes in the polymer matrix due to the high ability of these tubes to agglomerate. One of the techniques to improve the dispersion of CNTs in polymers is their chemical modification through covalent or noncovalent attachments of CNT functional groups with the matrix [25]. To enhance the CNT/polymer interactions, ILs have been commonly used. For example, conducting polychloroprene rubber composites were developed using 1-butyl-3-methylimidazolium bis(trifluoromethylsulfonyl)imide and multi-walled carbon nanotubes (MWCNTs). The cation-π-interactions between the ionic liquid and tubes resulted in improved dispersion and the formation of a percolating MWCNT network that significantly increased the conductivity of the rubber composite. It was believed that the bundles of MWCNTs were uniformly distributed due to the strengthening of filler-rubber interactions, as well as the reduction in the inter-tubular interactions between the tubes. This was confirmed by the Payne effect in the composite, which is associated with the network formation of exfoliated carbon nanotubes in the rubber matrix. This secondary aggregate network of filler is broken down with the increase in the strain amplitude, and as a consequence, a decrease in the storage module was observed in the dynamic mechanical analysis. Moreover, the ILs acted as a plasticizer, affecting the storage module of the composite [9, 26].

ILs have also been applied to ensure better compatibility and enhance the dispersibility of MWCNTs in a blend of solution-SBR and polybutadiene rubber [27]. The best activity was found for the ionic liquid with a double bond in the cation (AMICl). In this case, the best reinforcing effect of the MWCNTs toward the rubber blend was achieved. It was suggested that the double bond in the AMICl molecules was chemically linked with the diene rubber double bonds by sulfur bridges. Additionally, in the presence of AMICl, the nanotubes strongly adhered to the rubber phase and formed a special type of bound rubber aggregation. No agglomeration of the MWCNTs was observed, leading to a continuous percolation network that increased the electrical and mechanical performance of the composites. Moreover, dynamic behavior in the vicinity of the CNT surface was detected by observing an extra relaxation peak at a temperature of approximately 80 °C. It was hypothesized that AMICl, having a reactive double bond towards sulfur vulcanization, reacted with the other reactive sites of the diene rubber. In this way, relaxation of the bound rubber that was very close to the surface of the CNTs took place at higher temperatures. In general, the use of imidazolium ILs gives rise to new possibilities to develop CNT composites with commodity polymers such as polystyrene (PS). For example, 1-cetyl-2, 3-dimethylimidazolium tetrafluroborate was reported as an excellent compatibilizer for MWCNTs toward polystyrene [28]. This PS composite contained highly dispersed individual carbon nanotubes. However, the mixture of the MWCNTs and ionic liquid needed pretreatment at 185°C before it was added to the polymer; otherwise, the MWCNTs were hardly dispersed in the PS and formed large agglomerates. Evidence for π interactions between the nanotubes and the imidazolium cation of the ILs was also reported. Moreover, the 20 °C improvement in the thermal stability of the PS composites was also demonstrated, which was explained by the enhanced degree of dispersion of the carbon nanotubes in the polymer matrix and better interfacial bonding between them.

Regarding elastomer compounds, one of the most important solid additives is vulcanization activator. Zinc oxide is widely used as an activator of the vulcanization of unsaturated elastomers by sulfur. It increases the amount of bound sulfur and as a result improves the efficiency of the crosslinking system. Additionally, zinc oxide reduces the vulcanization time of rubber compounds and improves the processing and physical properties of vulcanizates. Despite the important role of zinc oxide in sulfur vulcanization, its concentration in rubber compounds must be restricted to at least below 2.5% because zinc oxide is classified as being toxic to aquatic life. The release of zinc from rubber products occurs during their manufacturing, use, and recycling or disposal in landfills. Therefore, over the past several years, human activity has caused a significant increase in the amount of zinc in the environment. Designed EU legislation regarding environmental protection requires a reduction in the use of zinc oxide and zinc-containing compounds in technology. For elastomer technology, the most important of these is the European Commission Directive 2003/105/EC, which dictates that rubber products containing more than 2.5% of zinc compounds are considered to be highly toxic to aquatic ecosystems. Thus, methods to reduce the amount of zinc oxide in elastomers have been widely studied. The possibilities of reducing the ZnO content by incorporating zinc with a higher chemical activity in the form of reactive zinc complexes has been reported [29]. The availability of zinc ions in a complex molecule is believed to be higher than that in ZnO crystals. It has been shown that the zinc oxide content in natural rubber or ethylene-propylene-diene elastomer compounds can be reduced to 2 phr without affecting their vulcanizate properties [30]. Further reduction requires the use of anti-reversion agents. Another demonstrated approach to reduce the amount of Zn^{2+}ions in rubber compounds is the deposition of zinc ions on the surface of layered aluminosilicate, which also could serve as a filler [31]. However, the crosslink density of vulcanizates was significantly lower due to the low content of zinc ions in the crosslinking system and their limited availability for interaction. According to Nieuwenhuizen [32], the ZnO surface acts as a catalytic reaction template by activating and joining reactants. Accelerator particles, sulfur, and fatty acids diffuse through the elastomer matrix and are adsorbed onto the ZnO surface, forming intermediate reactive complexes. Therefore, the contact between the ZnO particles and accelerators in the elastomer matrix should be maximized to enhance the efficiency of zinc oxide during vulcanization. This contact depends on the ZnO particle shape, size, and specific surface area. Therefore, to reduce the amount of ZnO in rubber compounds, we intend to apply nanosized zinc oxide. A reduction in the particle size results in an increase in the zinc oxide specific surface area, providing better contact between the zinc oxide, accelerators, and sulfur particles. However, the dispersion of zinc oxide particles in an elastomer is also very important for the activation of sulfur vulcanization. Unfortunately, zinc oxide exhibits a high tendency to agglomerate in the elastomer matrix because of its high surface energy [6, 33]. From a technological point of view, it is difficult to obtain a homogeneous dispersion of ZnO nanoparticles in elastomers. Because zinc oxide and vulcanization accelerators are insoluble in rubber, it is assumed that the crosslinking reactions occur in a two-phase system and are catalyzed by conventional phase transfer catalysts. ILs are thought to catalyze the interfacial reactions; therefore, they can be assumed to play the same role in the crosslinking process [11]. Traditionally, stearic acid is used to improve the dispersion of zinc oxide in the elastomer. A complex of zinc, an accelerator, and fatty acid is formed during the vulcanization and consists of a central zinc cation, two stearyl anions, and accelerator residues. This complex is strongly polar and also exhibits a tendency to agglomerate in the elastomer. The crosslinking efficiency depends on the mobility of zinc ions in the complex molecule and on the diffusion rate of the remaining components in the crosslinking system. Therefore, the application of ligands with higher degrees of solvation towards zinc cations than towards stearyl anions should improve the dispersion of the components of the crosslinking system in the elastomer matrix, which is a role that ILs could play [33].

Designing ILs with special and functional structures is of crucial importance in exploring novel dispersing agents for nanosized zinc oxide and silica in elastomer composites. ILs can be fabricated with a high efficiency, and their structure can be easily tailored using various commercially available and cheap raw materials. Our preliminary studies have shown that an improvement in the dispersion of ZnO nanoparticles due to the ILs reduced the zinc ion content in vulcanizates, according to European Commission Directive 2003/105/EC. ILs also reduced the vulcanization time of the rubber compounds significantly and increased the crosslink density of the vulcanizates. Applying alkylimidazolium chlorides and tetraalkylammonium bromides allowed for the production of vulcanizates with the amount of zinc oxide, sulfur, and MBT reduced to 1.3 phr. These vulcanizates exhibit tensile strengths comparable to those without a dispersing agent [33].

Therefore, in this work, we intended to apply long-chain alkylimidazolium salts of chlorides, bromides, tetrafluoroborates, and hexafluorophosphates to improve the dispersion degree of zinc oxide nanoparticles in the butadiene-styrene (SBR) and ethylene-propylene-diene elastomers (EPDM) and, as a result, increase its activity during crosslinking. Moreover, because of the catalytic activity of ILs during interfacial reactions, an increase in the crosslinking efficiency is expected. In these studies, ILs such as alkylimidazolium salts with decyl-, didecyl-, dodecyl-, octadecyl-, and hexadecyl-chains in the cation, together with nanosized zinc oxide, were used to develop elastomer composites with a reduced amount of vulcanization activator. Vulcanizates were filled with nanosized silica in order to improve their mechanical performance.

2. Experimental section

2.1. Materials

The butadiene-styrene elastomer (KER 1500) containing 22-25 wt % styrene was obtained from Synthos Dwory, Oswiecim (Poland). Its Mooney viscosity was (ML1+4 (100°C):46-54). It was vulcanized with sulfur (Siarkopol Tarnobrzeg, Poland) with microsized zinc oxide as the standard activator (ZnO, Aldrich, Germany). 2-mercaptobenzothiazole (MBT, Aldrich, Germany) and N-cyclohexyl-2-benzothiazolesulfenamide (CBS, Aldrich, Germany) were applied as accelerators.

Ionic Liquid	Symbol
1-Decyl-3-methylimidazolium chloride	DMICl
1-Decyl-3-methylimidazolium tetrafluoroborate	$DMIBF_4$
1, 3-Didecyl-2-methylimidazolium chloride	DIDMICl
1-Dodecyl-3-methylimidazolium chloride	DODMICl
1-Dodecyl-3-methylimidazolium bromide	DODMIBr
1-Dodecyl-3-methylimidazolium tetrafluoroborate	$DODMIBF_4$
1-Dodecyl-3-methylimidazolium hexafluorophosphate	$DODMIPF_6$
1-Hexadecyl-3-methylimidazolium chloride	HDMICl
1-Hexadecyl-3-methylimidazolium tetrafluoroborate	$HDMIBF_4$
1-Hexadecyl-3-methylimidazolium hexafluorophosphate	$HDMIPF_6$
1-Methyl-3-octadecylimidazolium chloride	MODICl
1-Methyl-3-octadecylimidazolium hexafluorophosphate	$MODIPF_6$

Table 1. Ionic liquids used in this study

The ethylene-propylene-diene elastomer (Buna 5450) containing 48-56 wt % ethylene and 3.7-4.9 wt % ethylidene norbornene was obtained from Lanxess (Germany). Its Mooney viscosity was (ML1+4 (125°C):41-51). It was vulcanized with sulfur (Siarkopol Tarnobrzeg, Poland) with microsized zinc oxide as the standard activator (ZnO, Aldrich, Germany). 2-mercaptobenzothiazole (MBT, Aldrich, Germany), tetramethylthiuram monosulfide (TMTM, Akrochem Corporation, USA) and zinc dibutyldithiocarbamate (ZDBC, Performance Additives, Malaysia) were applied as accelerators.

To reduce the amount of zinc ions in the rubber compounds, nanosized zinc oxide (nZnO, Nanostructured & Amorphous Materials, Inc., USA) was used as an alternative to microsized ZnO. Silica with a specific surface area of 380 m^2/g (Aerosil 380, Evonic Industries, Germany) was used as a filler. The ionic liquids given in Table 1 were obtained from IoLiTec (Germany).

2.2. Preparation and characterization of rubber compounds

Rubber compounds with the formulations given in Table 2 were prepared using a laboratory two-roll mill. The samples were cured at 160 °C until they developed a 90% increase in torque, as measured by a rotational rotorless rheometer. The kinetics of rubber compound vulcanization was studied using a DSC1 (Mettler Toledo) analyzer by decreasing the temperature from 25 to-100 °C at a rate of 10 °C/min and then heating to 250 °C with the same heating rate.

The crosslink densities (ν_T) of the vulcanizates were determined by their equilibrium swelling in toluene, based on the Flory-Rehner equation [34]. The Huggins parameter of the SBR-solvent interaction (χ) was calculated from the equation 1

$$\chi = 0.370 + 0.560V_r \tag{1}$$

where V_r is the volume fraction of elastomer in the swollen gel and for the EPDM-solvent interaction.

$$\chi = 0.425 + 0.340V_r \tag{2}$$

The tensile properties of the vulcanizates were measured according to the ISO-37 standard procedures using a ZWICK 1435 universal machine.

SBR (phr)		**EPDM(phr)**	
Elastomer	100	Elastomer	100
Sulfur	2	Sulfur	2.5
*ZnO	5	*ZnO	5
MBT	1	MBT	1
CBS	1	TMTM	1
Silica	30	ZDBC	1.5
Ionic liquid	1.5	Silica	30
-		Ionic liquid	1.5

Table 2. Composition of the SBR and EPDM-based rubber compounds (*2 phr of nanosized zinc oxide was used as an alternative to 5 phr of standard activator)

2.3. Dynamic-mechanical analysis

Dynamic-mechanical measurements were carried out in tension mode using a DMA/SDTA861^e analyzer (Mettler Toledo). Measurements of the dynamic moduli were performed over the temperature range of-80-100°C with a heating rate of 2°C/min, a frequency of 1 Hz, and a strain amplitude of 4 μm. The temperature of the elastomer glass transition was determined from the maximum of tan δ=f(T), where tan δ is the loss factor and T is the measurement temperature.

2.4. Scanning Electron Microscopy (SEM)

The degree of dispersion of crosslinking agents and filler nanoparticles in the elastomer matrix was estimated using scanning electron microscopy with a LEO 1530 SEM. The vulcanizates were broken down in liquid nitrogen and the surfaces of the vulcanizate fractures were examined. Prior to the measurements, the samples were coated with carbon.

2.5. Thermogravimetric analysis

The thermal stability of the vulcanizates was studied using a TGA/DSC1 (Mettler Toledo) analyzer. Samples were heated from 25 °C to 700 °C in an argon atmosphere (60 ml/min) with a heating rate of 10 °C/min. Decomposition temperatures at a weight loss of 2% (T_{02}), 5% (T_{05}), 50% (T_{50}), and the total weight loss during decomposition of the vulcanizates were determined.

2.6. Thermo-oxidative and UV aging

The thermo-oxidative degradation of the vulcanizates was performed at a temperature of 100 °C for 240 h. The UV degradation of the vulcanizates was carried out for 120 h using a UV 2000 (Atlas) machine in two alternating segments: a day segment (irradiation 0.7 W/m^2, temperature 60 °C, time 8 h) and a night segment (without UV radiation, temperature 50 °C, time 4 h).

To estimate the resistance of the samples to aging, their mechanical properties and crosslink densities after aging were determined and compared with the values obtained for the vulcanizates before the aging process. The aging factor (S) was calculated as the numerical change in the mechanical properties of the samples upon aging (Equation 3) [35], where TS is the tensile strength of the vulcanizates and EB is the elongation at break:

$$S = \left(TS \cdot EB\right)_{\text{after aging}} \Big/ \left(TS \cdot EB\right)_{\text{before aging}} \tag{3}$$

3. Results and discussion

3.1. SBR composites containing ILs

Dispersion degree of activator and filler nanoparticles in the SBR

The degree of dispersion of zinc oxide nanoparticles in the elastomer matrix is very important to the activation of sulfur vulcanization. Homogeneous dispersion of ZnO nanoparticles provides better contact between the activator and other components of the crosslinking system and, as a consequence, enhances the efficiency of zinc oxide during vulcanization. SEM images were taken to estimate the dispersion degree of zinc oxide particles in the elastomer in the presence of ILs (Figures 1-6).

The zinc oxide nanoparticles (Figure 1) are not homogeneously distributed in the SBR. They create microsized agglomerates with different shapes, consisting of nanosized primary particles. The high tendency of ZnO particles to agglomerate results from their high surface energy and ability for specific interactions [6]. The agglomeration of zinc oxide particles causes their surface area to decrease, followed by a decrease in the interface between the ZnO, accelerator, and sulfur particles. As a result, the efficiency of elastomer crosslinking decreases. In general, the ILs improved the dispersibility of ZnO and silica nanoparticles in the SBR, but to different degrees. Homogeneous dispersion of the nanoparticles was achieved for DMICl, DODMIBF$_4$, and MODIPF$_6$. These ILs seemed to be the best dispersing agents, which effectively prevented ZnO and filler nanoparticles from agglomeration. In the case of HDMICl-and MODICl-containing vulcanizates, some agglomerates of nanoparticles can be seen; however, they are of smaller size and better elastomer wettability than those observed for the vulcanizates without IL. The different effect of ILs on the dispersibility of nanoparticles in the elastomer matrices could result from their different miscibilities with the elastomers during the preparation of rubber compounds. For example, HDMICl and MODICl exhibited poorer miscibility with SBR than other ILs and caused elastomer crumbling during the preparation of rubber compounds.

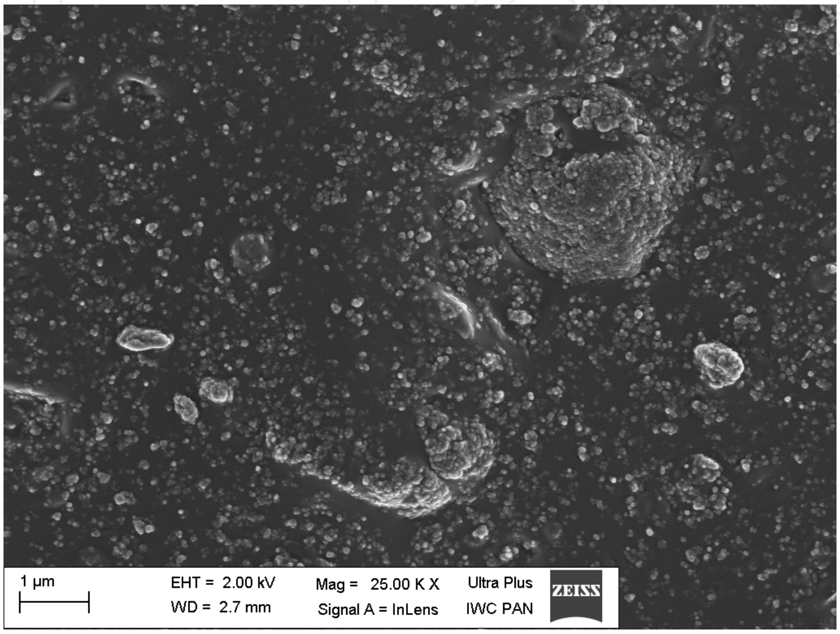

Figure 1. SEM image of SBR vulcanizates containing NZnO without IL

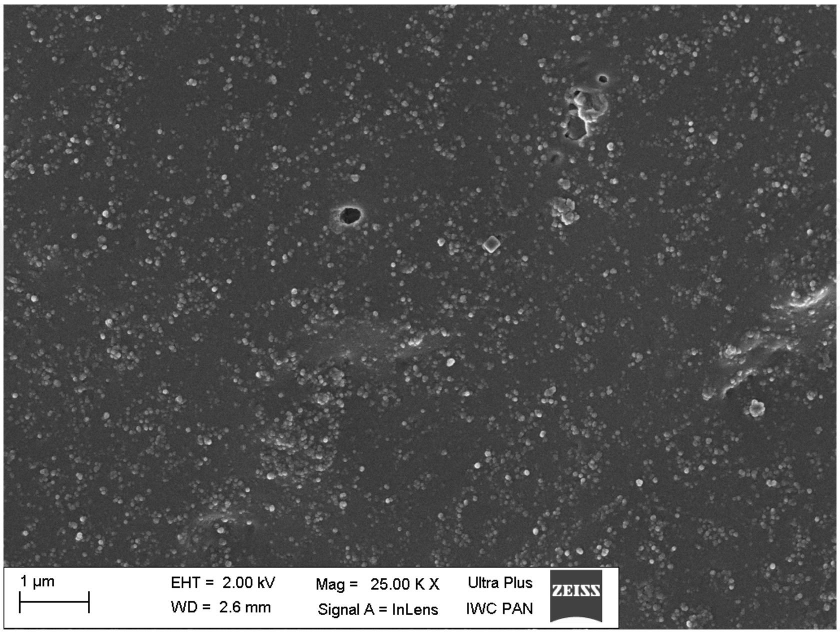

Figure 2. SEM image of SBR vulcanizates containing NZnO and DMICl

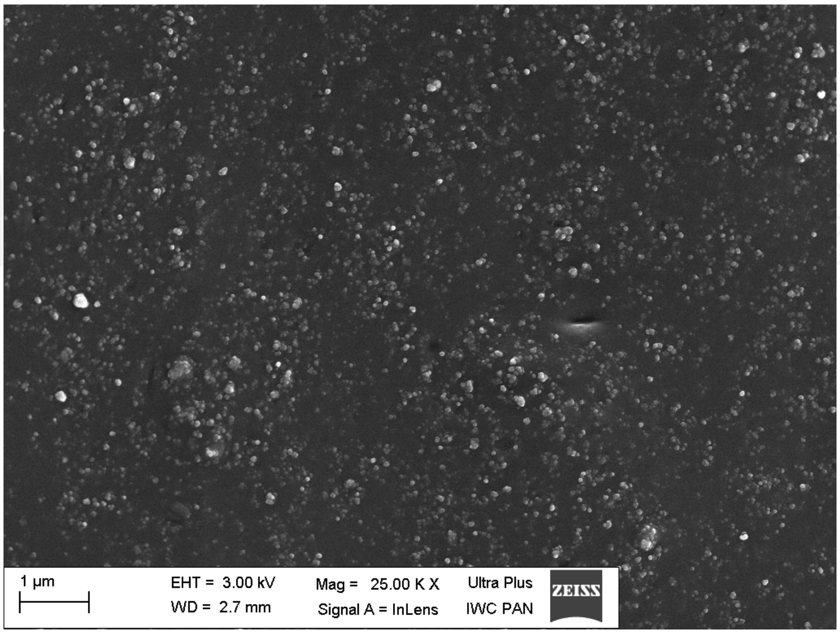

Figure 3. SEM image of SBR vulcanizates containing NZnO and DODMIBF_4

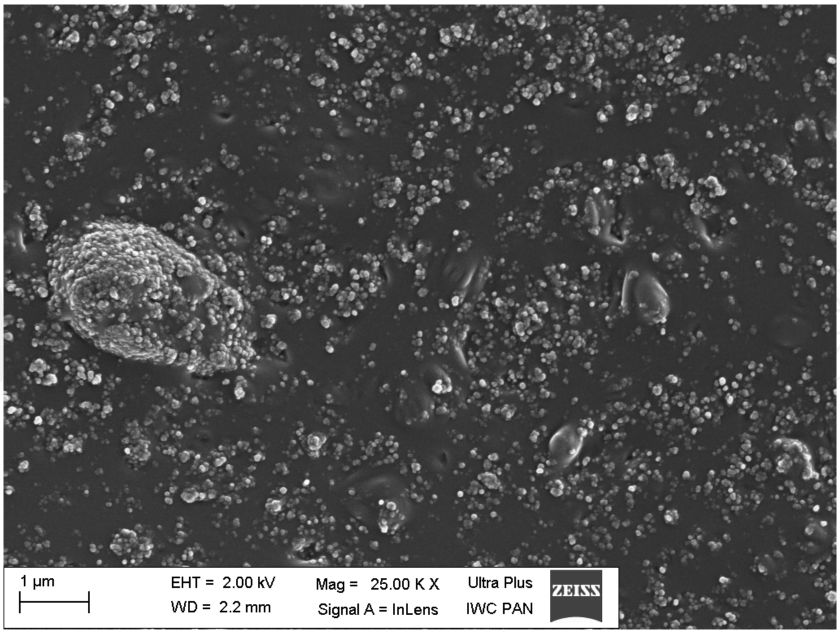

Figure 4. SEM image of SBR vulcanizates containing NZnO and HDMICl

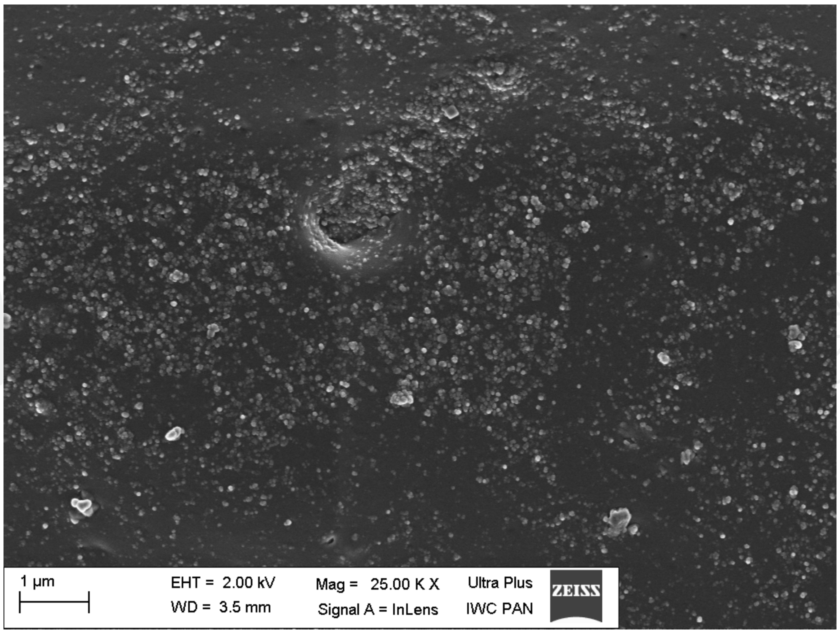

Figure 5. SEM image of SBR vulcanizates containing NZnO and MODICl

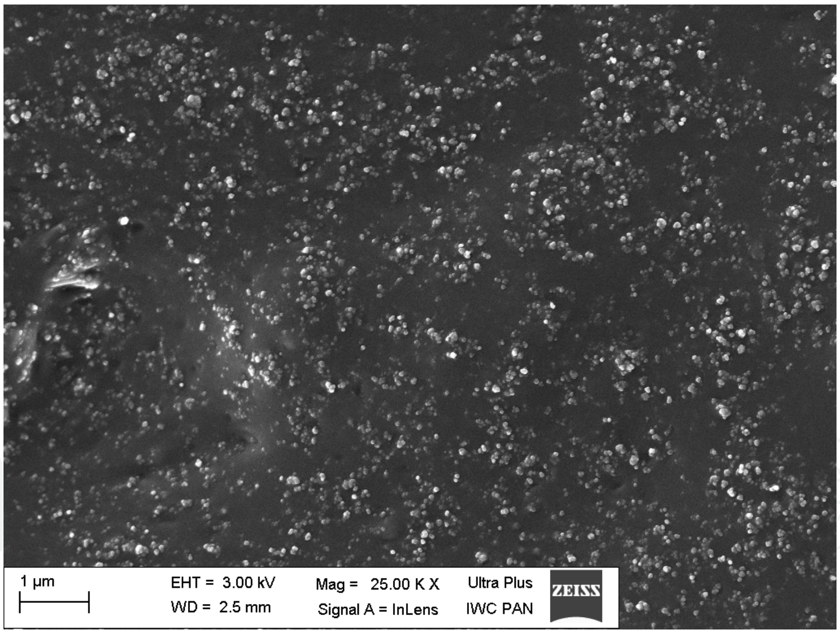

Figure 6. SEM image of SBR vulcanizates containing NZnO and MODIPF$_6$

Curing characteristics and the crosslink density of SBR vulcanizates

Because the ILs improved the degree of dispersion of the activator nanoparticles and are considered to catalyze the interface reactions, they should affect the vulcanization efficiency of SBR compounds. The influence of the ILs on the vulcanization process was estimated based on rheometer measurements. The cure characteristics of SBR compounds and crosslink densities of vulcanizates are given in Table 3.

The nanosized zinc oxide used alternatively to microsized activator increased the crosslink density of the vulcanizates and, as a result, the torque increment during the vulcanization of the rubber compounds. It also decreased the vulcanization time of the SBR compounds by 10 minutes and reduced the scorch time by a factor of two. Applying ILs resulted in a considerably shorter vulcanization time compared with micro-or nano-ZnO systems. This confirms that ILs act as catalysts of interface crosslinking reactions. The influence of the anion present in the ILs on the vulcanization time was also observed: the shortest cure times were exhibited by rubber compounds containing alkylimidazolium tetrafluoroborates, whereas the longest t_{90} values were observed for rubber compounds with alkylimidazolium bromide and chlorides. The length of the alkyl chains in the ILs did not significantly affect the torque increment of the rubber compounds during vulcanization. There was also no correlation between the length of the IL alkyl chains and the vulcanization time. However, the length of the alkyl chains in the imidazolium cation seemed to have an impact on the crosslink density. The highest crosslink densities were exhibited by the elastomer compounds with 1-hexadecyl-3-methylimidazolium salts.

ILs	**ΔG (dNm)**	**t_{90} (min)**	**t_p (min)**	**$\nu_T * 10^4$(mol/cm^3)**
ZnO	18.8	60	0.7	15.4
NZnO	20.8	50	0.3	16.5
DMICl	21.5	36	0.5	17.9
DMIBF$_4$	20.6	29	0.5	17.7
DIDMICl	20.6	27	0.5	17.3
DODMICl	22.2	33	0.5	16.9
DODMIBr	22.4	40	0.5	17.4
DODMIBF$_4$	19.8	24	0.5	17.4
DODMIPF$_6$	19.4	27	0.5	17.1
HDMICl	19.5	30	0.5	18.4
HDMIBF$_4$	20.2	25	0.5	20.0
HDMIPF$_6$	19.8	29	0.4	18.1
MODICl	18.9	36	0.5	17.8
MODIPF$_6$	20.6	32	0.6	18.2

Table 3. Curing characteristics and crosslink densities of SBR vulcanizates (ΔG-increment of torque in the rubber compound during vulcanization; t_{90}-optimal vulcanization time; t_p-scorch time, ν_T – crosslink density of vulcanizates)

Having studied the effect of nanosized zinc oxide and ILs on the curing characteristics of SBR compounds, we then examined their influence on the temperature and energetic effects of vulcanization using DSC analysis. The results for SBR compounds are given in Table 4.

The vulcanization of SBR is an exothermic process that takes place in a temperature range of 179-232 °C, with an energetic effect of 10 J/g. Nanosized zinc oxide had no significant influence on the temperature and heat of vulcanization compared with those of the SBR compounds containing microsized ZnO. However, it is worth noting that ILs decreased the vulcanization onset temperature by 30°C compared with rubber compounds with micro-or nanosized activator. This is important for technological reasons because application of these ILs allows the SBR elastomer to be cured at lower temperatures than the commonly used 160°C. The highest onset vulcanization temperatures were achieved for hexafluorophosphates, whereas the lowest were observed for alkylimidazolium chlorides. ILs decreased the energetic effect of vulcanization, particularly hexafluorophosphates. The influence of the cations was also observed: the energetic effect of vulcanization was the lowest for rubber compounds containing ILs with 1-hexadecyl-3-methylimidazolium and 1-methyl-3-octadecylimidazolium cations.

ILs	Vulcanization temperature range	Energetic effect of vulcanization
	(°C)	(J/g)
ZnO	179-232	10.0
NZnO	181-226	9.1
DMICl	148-239	8.4
$DMIBF_4$	149-234	7.6
DIDMICl	148-239	9.0
DODMICl	148-241	9.9
DODMIBr	149-239	7.7
$DODMIBF_4$	148-235	6.5
$DODMIPF_6$	154-233	6.7
HDMICl	150-223	6.4
$HDMIBF_4$	150-233	6.4
$HDMIPF_6$	154-230	5.3
MODICl	145-236	5.6
$MODIPF_6$	157-233	4.7

Table 4. Temperature and energetic effects of SBR vulcanization measured by DSC

Mechanical properties of SBR vulcanizates

The aim of applying the ILs was to achieve a homogeneous dispersion of the zinc oxide and silica nanoparticles in the elastomer and thereby improve the mechanical properties of the vulcanizates, such as the tensile strength. Agglomerates of zinc oxide particles may be responsible for local increases in the crosslink density of vulcanizates and the formation of densely crosslinked domains with low elasticity, which may initiate breaking of the sample under external stress. Filler nanoparticle agglomerates can also concentrate stress and contribute to a deterioration of the strength parameters of the vulcanizates.

The mechanical properties of the SBR vulcanizates were studied under static and dynamic conditions. The results of the tensile tests are presented in Table 5.

ILs	TS (MPa)	EB (%)
ZnO	18.3	777
NZnO	22.4	781
DMICl	29.1	964
$DMIBF_4$	28.5	982
DIDMICl	26.1	962
DODMICl	24.2	889
DODMIBr	29.8	954
$DODMIBF_4$	27.2	985
$DODMIPF_6$	22.1	973
HDMICl	20.7	972
$HDMIBF_4$	22.5	915
$HDMIPF_6$	26.5	987
MODICl	21.5	946
$MODIPF_6$	24.8	989

Table 5. Tensile strengths (TS) and elongation at breaks (EB) of the SBR vulcanizates

SBR crosslinked with microsized zinc oxide used as a vulcanization activator exhibited a tensile strength of 18.3 MPa and an elongation at break of approximately 777%. Nanosized zinc oxide increased the tensile strength of vulcanizate by 4 MPa, whereas the elongation at break did not change. ILs caused a further increase in the tensile strengths of the vulcanizates. This effect was most significant for vulcanizates containing ILs with decyl-, didecyl-, and dodecyl-chains in the cation. It should be noted that these ILs allowed for a homogeneous dispersion of ZnO and filler nanoparticles in the SBR elastomer. The lowest tensile strengths were exhibited for vulcanizates with HDMICl and MODICl due to the poor dispersion of nanoparticles in the elastomer matrix.

In addition to the mechanical properties under static conditions, the dynamic mechanical properties are also important for the technological application of rubber products. The influence of ILs on the loss factor (tan δ) was determined with DMA. The loss factor is a measure of the material ability to dampen vibration. A plot of tan δ as a function of temperature for the vulcanizates containing ILs is presented in Figure 7, and the data are also shown in Table 6. The presence of the glass transition of the SBR elastomer can be observed, with a maximum that represents the glass transition temperature T_g.

ILs	T_g (°C)	tan δ at T_g (-)	tan δ at 25 °C (-)	tan δ at 100 °C (-)
ZnO	-40.9	0.58	0.13	0.09
NZnO	-40.1	0.63	0.13	0.09
DMICl	-37.3	0.70	0.11	0.08
$DMIBF_4$	-35.1	0.86	0.09	0.07
DODMIBr	-36.4	0.74	0.13	0.10
$DODMIBF_4$	-38.0	0.76	0.09	0.06
$HDMIPF_6$	-36.9	0.68	0.12	0.10
$MODIPF_6$	-35.1	0.73	0.13	0.10

Table 6. Glass transition temperature (T_g) and loss factor (tan δ) of SBR vulcanizates

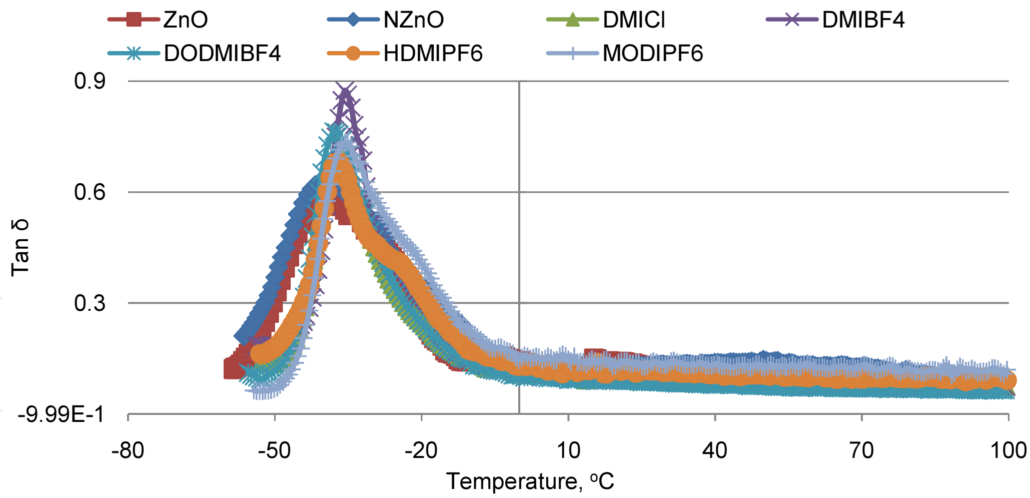

Figure 7. Loss factor (tan δ) versus temperature for SBR vulcanizates

Applying nanosized ZnO had no influence on the glass transition temperature of SBR and the values of the loss factor. However, an increase in the T_g of the vulcanizates was observed when using ILs, which was the result of the crosslink density increase. The densely crosslinked elastomer network that was formed during vulcanization restricted the mobility of the SBR chains. Regarding the loss factor, tetrafluoroborates increased the value of tan δ at T_g but decreased the loss factor at room temperature and elevated temperatures. Other ILs slightly increased the values of the loss factor at the glass transition temperature but had no significant effect on tan δ at 25 °C and 100 °C. Considering the magnitude of the change in the value of loss factor, it can be concluded that the use of ILs had no significant effect on the ability of vulcanizates toward vibration damping. In addition, vulcanizates exhibited stable dynamic properties at the temperatures studied.

Thermal stability and aging resistance of SBR vulcanizates

Thermal stability is very important for the technological application of rubber products. Therefore, ILs used to improve the degree of dispersion of zinc oxide and silica in the elastomer should not deteriorate this property. The thermal stabilities of the vulcanizates were examined based on their decomposition temperature and the total weight loss of the sample determined by TGA analysis. The results are presented in Table 7.

The thermal decomposition of SBR containing microsized zinc oxide began at 288 °C. Replacing the standard activator with nanosized zinc oxide improved the thermal stability of SBR. The decomposition of the vulcanizate began at a temperature that was 15 °C higher than that of the reference vulcanizate. The use of ILs caused a further increase in the thermal stability of SBR, likely due to the homogeneous dispersion of the nanoparticles in the elastomer matrix. The highest T_{02} temperature was achieved for vulcanizates with DMICl and $DMIBF_4$, where filler and activator nanoparticles were the most uniformly distributed in the SBR. The network created by the filler nanoparticles may be a barrier for the transport of gases and volatile pyrolysis products, thus increasing the thermal stability of the composite. Additionally, ILs did not affect the temperatures at 5% and 50% weight loss. A 5% weight loss was achieved in the temperature range of 357-361 °C, and a 50% weight loss occurred at 441-442 °C. The total weight loss during decomposition was similar for all vulcanizates and was in the range of 74-77%.

ILs	T_{02} (°C)	T_{05} (°C)	T_{50} (°C)	Total weight loss (%)
ZnO	288	362	442	74.2
NZnO	303	360	442	76.9
DMICl	320	362	442	75.6
$DMIBF_4$	314	360	444	75.5
DODMIBr	318	361	441	76.0
$DODMIBF_4$	314	361	444	75.3
$HDMIPF_6$	306	357	442	75.0
$MODIPF_6$	306	357	441	75.3

Table 7. Decomposition temperatures at a weight loss of 2% (T_{02}), 5% (T_{05}), 50% (T_{50}), and total weight loss during the decomposition of SBR vulcanizates

One of the most important properties of rubber products is their aging resistance. Therefore, the effect of nanosized zinc oxide and ILs on vulcanizate resistance to UV and thermo-oxidative aging was examined through the change in their mechanical properties and crosslink density.

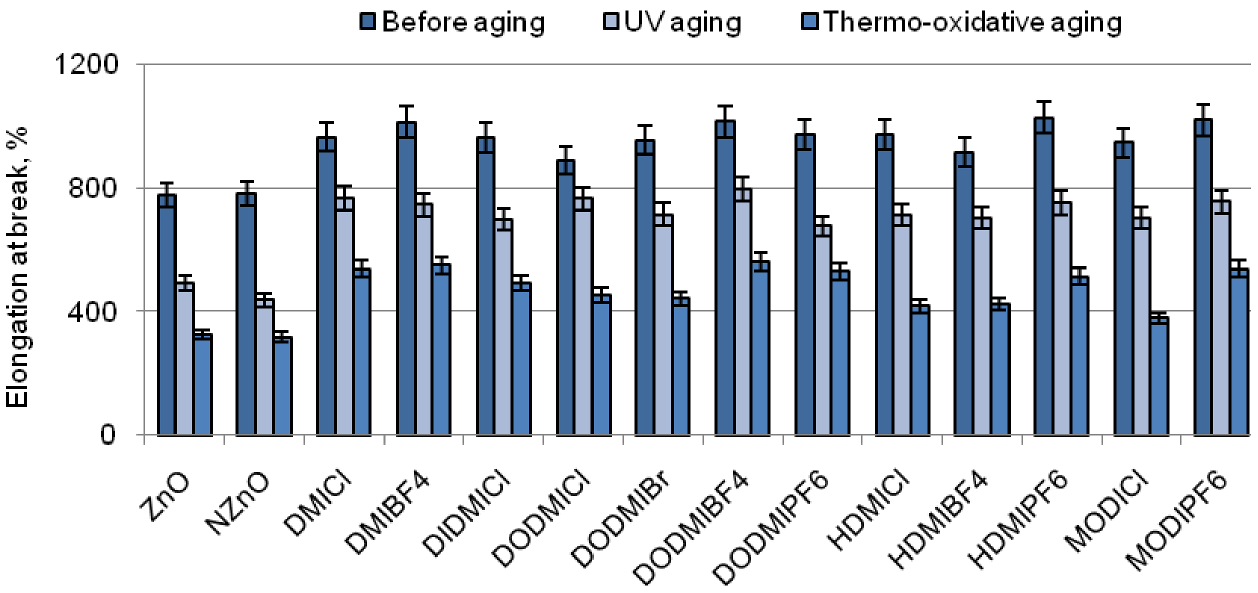

Figure 8. Elongation at breaks of SBR vulcanizates after aging

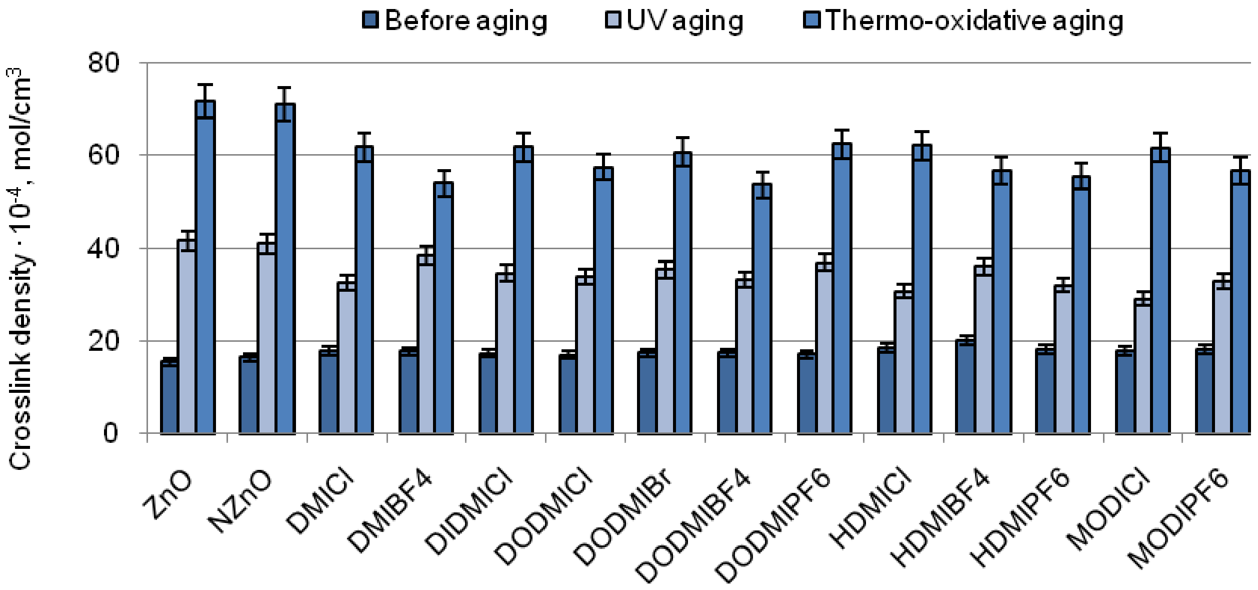

Figure 9. Crosslink densities of SBR vulcanizates after aging

In Figure 8, the change in elongation at break upon aging is given for SBR vulcanizates. The aging process had a considerable impact on the elongation at break of vulcanizates, causing it to decrease by approximately 200% for UV aging and 300-400% for thermo-oxidative aging. These changes reflect the large increase in the crosslink density of the vulcanizates. Under the influence of aging factors such as UV radiation and elevated temperature, further crosslinking of the elastomer took place. In the case of vulcanizates containing ILs, the extent of further crosslinking of the elastomer was greatly reduced (Figure 9). UV radiation caused a twofold increase in the crosslink density of the vulcanizates, while in the case of the thermo-oxidative aging, a threefold increase in the crosslink density was observed. Due to the considerable changes in the crosslink density of SBR vulcanizates, the aging process deteriorated their tensile strength. The smallest change in the tensile strength was achieved for the vulcanizate containing DODMIPF$_6$ and MODICl (Figure 10).

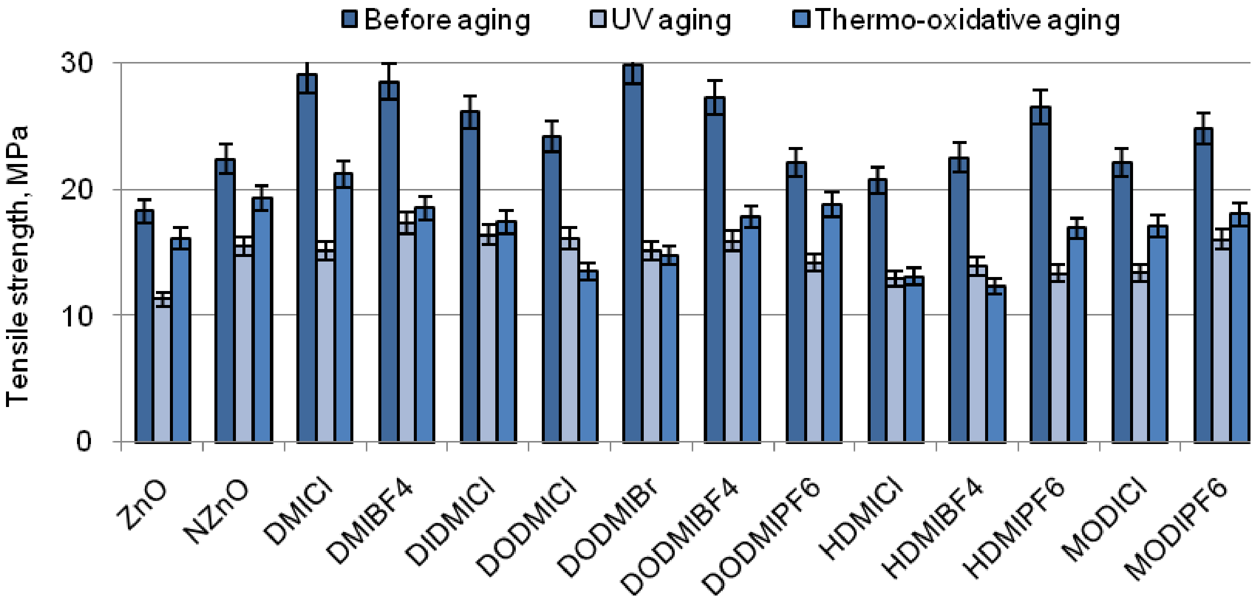

Figure 10. Tensile strengths of SBR vulcanizates after aging

To quantitatively estimate the change in the mechanical properties of vulcanizates due to aging, the aging factor S was calculated (Table 8). This factor is a measurement of the changes in the sample deformation energy caused by the aging process. Values of the S-factor that are closer to 1 indicate smaller changes in the mechanical properties of the vulcanizates from the aging process.

The aging factor (S) for vulcanizates without ILs is 0.39 (UV aging) and 0.35 (thermo-oxidative aging). Therefore, it can be concluded that the SBR vulcanizates are characterized by a susceptibility to degradation under prolonged exposure to elevated temperature or UV radiation. The application of ILs did not significantly improve the resistance of SBR to UV aging. The highest values of S_{UV} were observed for the vulcanizates containing DODMICl and HDMICl, which were 0.57 and 0.51, respectively. These ILs provided the best protection for SBR against UV aging. No improvement in the SBR resistance to thermo-oxidative aging was observed.

ILs	S_{UV} (-)	S_T (-)
ZnO	0.39	0.35
NZnO	0.39	0.35
DMICl	0.41	0.41
$DMIBF_4$	0.45	0.35
DIDMICl	0.46	0.34
DODMICl	0.57	0.28
DODMIBr	0.38	0.23
$DODMIBF_4$	0.46	0.36
$DODMIPF_6$	0.45	0.39
HDMICl	0.51	0.30
$HDMIBF_4$	0.47	0.25
$HDMIPF_6$	0.37	0.32
MODICl	0.45	0.32
$MODIPF_6$	0.48	0.38

Table 8. UV and thermo-oxidative aging factors for SBR vulcanizates

3.2. EPDM composites containing ILs

Dispersion degree of activator and filler nanoparticles in the EPDM

Having established the effects of nanosized zinc oxide and ILs on the SBR properties, we then examined the EPDM vulcanizates. EPDM is widely applied to manufacture rubber products for the automotive industry (tires and damping elements) and the building industry (sealing profiles) due to its useful properties such as resistance to ozone and elevated temperature and elasticity at low temperatures. Therefore, it is reasonable to search for new substances to improve the degree of dispersion of zinc oxide and silica nanoparticles in EPDM elastomer.

As expected, zinc oxide and filler nanoparticles were not homogeneously distributed in the EPDM elastomer matrix, and poor dispersion was observed. They created microsized agglomerates with complex structures, as shown in Figure 11. The size of the agglomerates was several micrometers, whereas the primary particles were below 300 nm in size. Moreover, the agglomerates displayed poor adhesion to the elastomer. We found that ILs prevented the nanoparticles from agglomeration, with the most effective being alkylimidazolium chlorides and bromides, which allowed for a homogeneous distribution of nanoparticles in the EPDM elastomer (Figures 12, 13, 15). In the case of tetrafluoroborates, some agglomerates are observed in the SEM images. However, they are smaller in size and exhibit better adhesion to the elastomer than for the vulcanizate without ILs (Figures 14, 16). Therefore, it can be concluded that the efficiency of ILs as dispersing agents in EPDM depends mainly on the anion type and not the length of alkyl chains in the imidazolium cation.

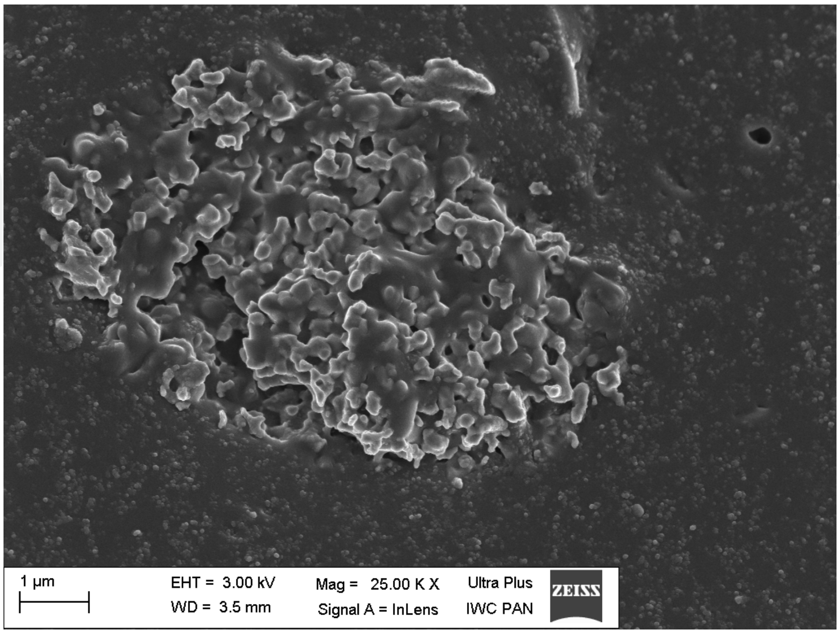

Figure 11. SEM images of SBR vulcanizates containing NZnO without IL

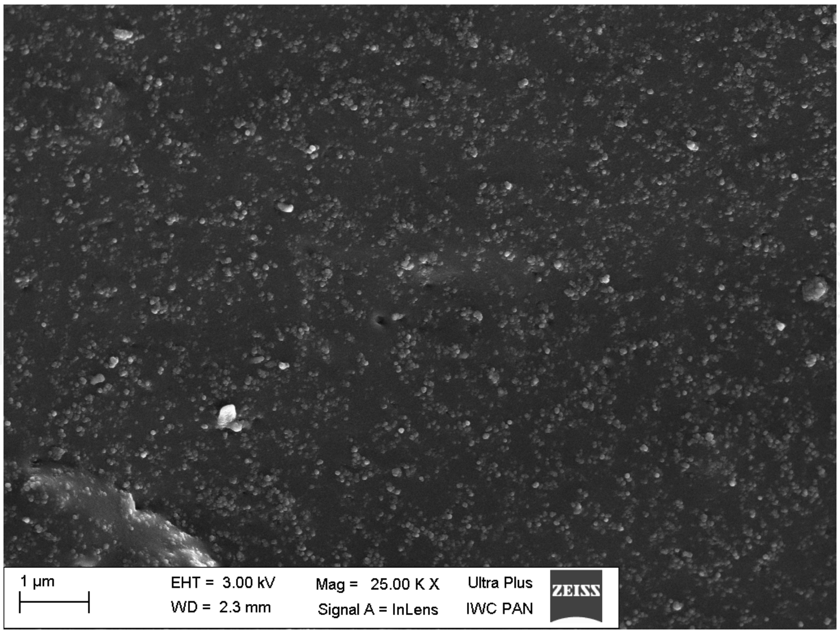

Figure 12. SEM images of SBR vulcanizates containing NZnO and DODMIBr

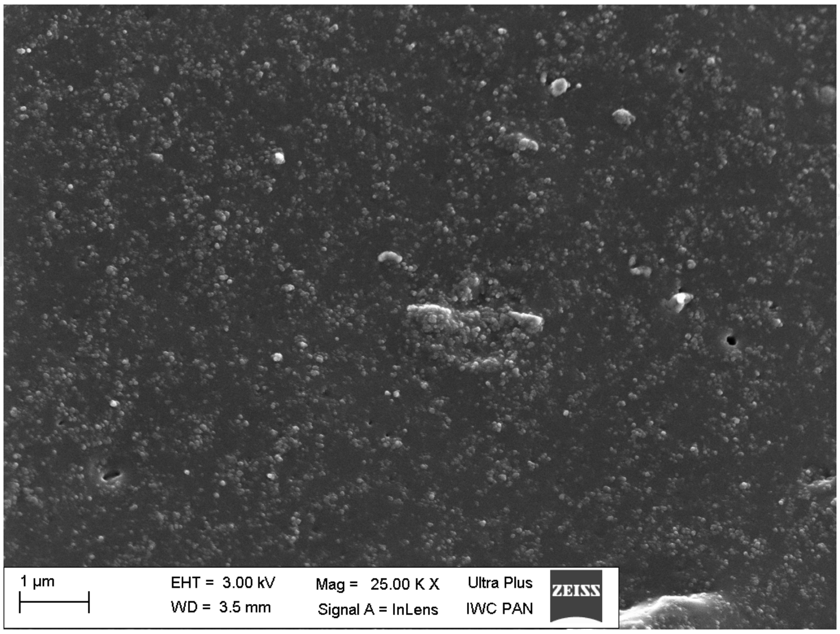

Figure 13. SEM images of SBR vulcanizates containing NZnO and DMICl

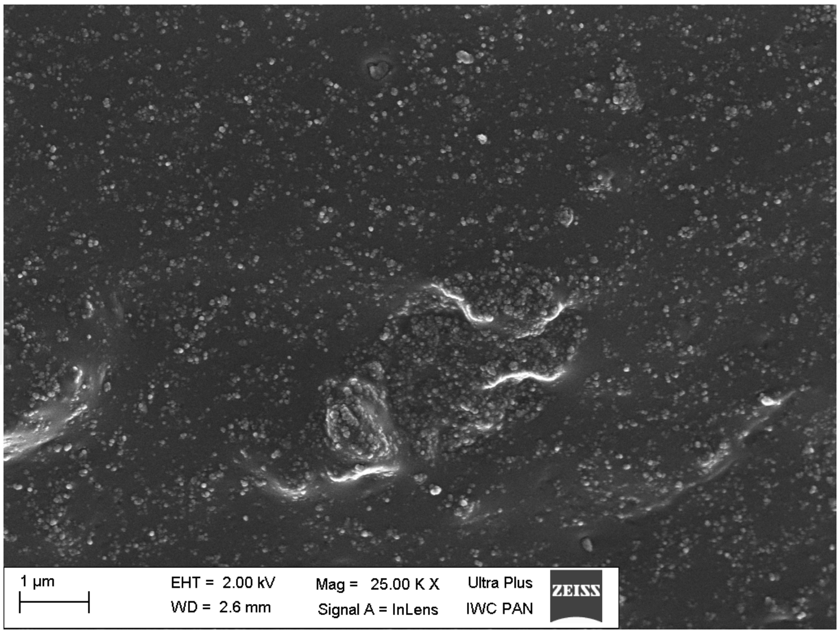

Figure 14. SEM images of SBR vulcanizates containing NZnO and DMIBF$_4$

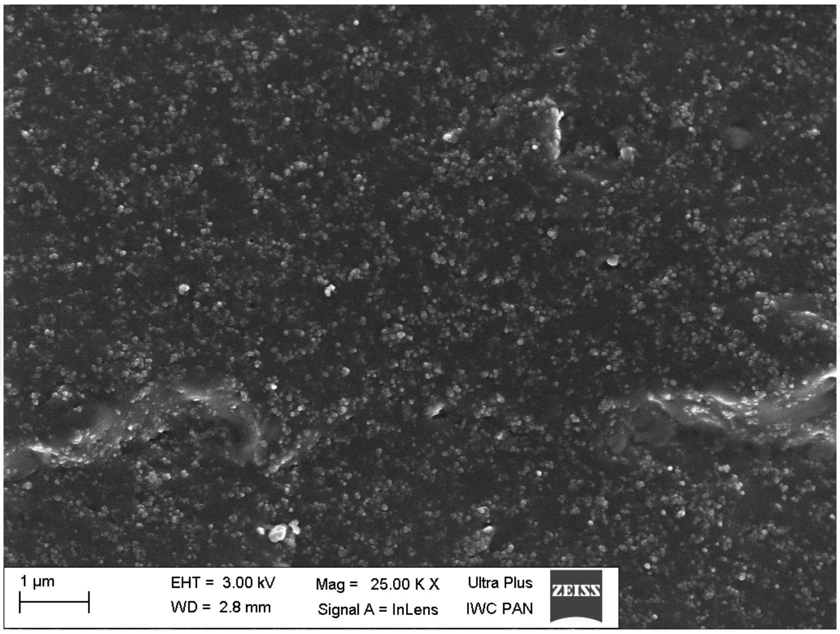

Figure 15. SEM images of SBR vulcanizates containing NZnO and HDMICl

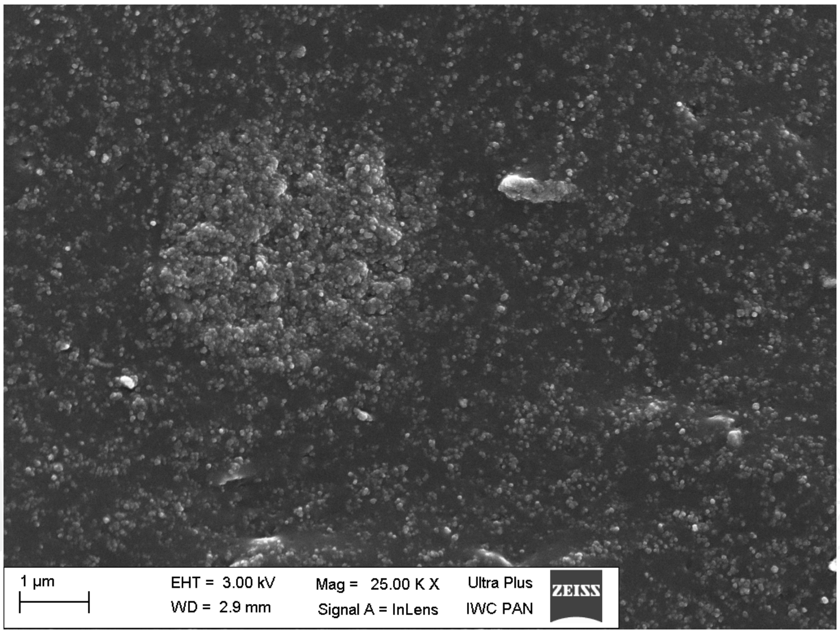

Figure 16. SEM images of SBR vulcanizates containing NZnO and $HDMIBF_4$

Curing characteristics and the crosslink density of EPDM vulcanizates

Rheometric measurements were performed to study the effect of nanosized zinc oxide and ILs on the torque increment during vulcanization, which corresponds to the crosslinking degree of the elastomer. The vulcanization times and scorch times were also determined (Table 9).

Replacing 5 phr of microsized zinc oxide with 2 phr of zinc oxide nanoparticles increased the torque increment during vulcanization and therefore the crosslink density of vulcanizates, despite the reduction in the amount of zinc oxide in the rubber compound. As discussed, this reduction is important for ecological reasons. There was no considerable effect on the vulcanization time or scorch time observed. ILs caused a further increase in the crosslink densities of the vulcanizate and, as a consequence, the torque increment during vulcanization. It should be noticed that the highest crosslink densities were achieved for vulcanizates containing alkylimidazolium bromide and chlorides, which provided a homogeneous dispersion of zinc oxide nanoparticles in the elastomer. As a result, the interface between the activator particles and other components of the crosslinking system increased, improving the efficiency of the vulcanization process. Regarding the cation type of IL, the lowest crosslink densities were observed for vulcanizates containing 1-methyl-3-octadecylimidazolium cation. ILs, especially those with decyl-, didecyl-, and dodecyl-chains, reduced the vulcanization time of rubber compounds. A small reduction in the scorch times was also observed, but it was not of technological significance.

ILs	**ΔG (dNm)**	**t_{90} (min)**	**t_p (s)**	**$\nu_T * 10^5$(mol/cm^3)**
ZnO	16.5	40	50	9.3
NZnO	18.0	38	45	10.6
DMICl	20.4	25	36	14.0
$DMIBF_4$	21.0	28	32	12.2
DIDMICl	20.8	28	35	13.5
DODMICl	23.1	25	39	14.6
DODMIBr	22.0	30	35	14.0
$DODMIBF_4$	20.0	30	33	12.0
$DODMIPF_6$	21.4	36	38	14.1
HDMICl	22.7	33	42	14.7
$HDMIBF_4$	18.5	33	38	12.1
$HDMIPF_6$	21.2	35	40	12.2
MODICl	18.9	30	42	12.1
$MODIPF_6$	20.4	32	42	11.3

Table 9. Curing characteristics and crosslink densities of EPDM vulcanizates (ΔG-increment of torque in the rubber compound during vulcanization; t_{90}-optimal vulcanization time; t_p-scorch time, ν_T – crosslink density of vulcanizates)

Using DSC, we determined the vulcanization temperature range and the energetic effect of vulcanization for the rubber compounds (Table 10).

IL	Vulcanization temperature range (°C)	Energetic effect of vulcanization (J/g)
ZnO	133-193	10.3
NZnO	139-199	9.8
DMICl	112-229	7.4
$DMIBF_4$	114-228	6.8
DIDMICl	110-225	7.4
DODMICl	112-229	8.5
DODMIBr	114-239	7.2
$DODMIBF_4$	120-234	8.3
$DODMIPF_6$	112-223	8.4
HDMICl	120-226	6.5
$HDMIBF_4$	121-232	6.4
$HDMIPF_6$	120-224	7.4
MODICl	142-227	4.4
$MODIPF_6$	139-223	4.7

Table 10. Temperature and energetic effects of EPDM vulcanization measured by DSC

The vulcanization of EPDM is an exothermic process that takes place in the temperature range of 133-193°C, with an energetic effect of 10.3 J/g for microsized ZnO. Nanosized activator had no significant influence on the temperature and heat of vulcanization compared with the microsized ZnO. The catalytic effect of ILs on the interface crosslinking reactions is also apparent in the case of EPDM. ILs decreased the vulcanization onset temperature by 20-30°C and the energetic effect of vulcanization compared with rubber compounds without alkylimidazolium salts. Exeptions are ILs with 1-methyl-3-octadecylimidazolium cation, which did not influence the vulcanization temperature. However, they considerably decreased the energetic effect of vulcanization and therefore the vulcanization efficiency. It should be mentioned that in the case of these ILs, the smallest crosslink densities of EPDM vulcanizates were also achieved.

Mechanical properties of EPDM vulcanizates

Having established the effect of alkylimidazolium salts on the degree of dispersion of zinc oxide and silica nanoparticles in the elastomer and on the crosslink density of vulcanizates, we then examined the mechanical properties of EPDM vulcanizates (Table 11).

Applying nanosized zinc oxide alternatively to the corresponding microsized activator decreased the tensile strength of the vulcanizate. This was likely due to the agglomeration of nanoparticles in the EPDM. Agglomerates with poor wettability with the elastomer can concentrate stress during deformation, resulting in the destruction of the sample. The increase in the tensile strength of vulcanizates containing ILs is closely related to the improvement of the degree of dispersion of the nanoparticles in the EPDM and to the increase in the crosslink density of the vulcanizates. The more uniform the dispersion of nanoparticles is in the elastomer, which results in a higher the crosslink density of the vulcanizates, the higher their tensile strength. In general, ILs increased the elongation at break of vulcanizates due to the increase in their elasticity.

ILs	TS (MPa)	EB (%)
ZnO	13.4	529
NZnO	10.7	569
DMICl	20.7	690
$DMIBF_4$	13.4	566
DIDMICl	19.5	667
DODMICl	25.1	735
DODMIBr	22.1	715
$DODMIBF_4$	13.2	528
$DODMIPF_6$	18.6	643
HDMICl	19.5	765
$HDMIBF_4$	12.5	581
$HDMIPF_6$	16.6	690
MODICl	19.6	778
$MODIPF_6$	18.3	702

Table 11. Tensile strengths (TS) and elongation at breaks (EB) of EPDM vulcanizates

The influence of ILs on the dynamic mechanical properties was determined with DMA. The loss factor as a function of temperature for the EPDM vulcanizates containing ILs is presented in Table 12. Measurements were performed for vulcanizates containing alkylimidazolium chlorides.

The determined glass transition temperatures for the vulcanizates with microsized and nanosized ZnO were approximately-45.4°C and-44.0°C, respectively, whereas the T_g value was slightly higher for the vulcanizates with ILs. This was likely due to the higher crosslink densities of the vulcanizates containing ILs. Nanosized zinc oxide and ILs did not considerably affect the values of the loss factor (tan δ). Therefore, it can be concluded that vulcanizates with ILs exhibit damping properties comparable to the reference sample containing microsized ZnO.

ILs	T_g (°C)	tan δ at T_g (-)	tan δ at 25 °C (-)	tan δ at 100 °C (-)
ZnO	-45.4	0.56	0.08	0.09
NZnO	-44.0	0.60	0.10	0.09
DMICl	-42.1	0.52	0.11	0.09
DIDMICl	-41.8	0.55	0.10	0.10
DODMICl	-43.5	0.58	0.09	0.09
HDMICl	-43.3	0.66	0.10	0.08
MODICl	-39.3	0.49	0.08	0.09

Table 12. Glass transition temperatures (T_g) and loss factors (tan δ) of EPDM vulcanizates

Thermal stability and aging resistance of EPDM vulcanizates

TGA analysis was performed to determine the effect of nanosized zinc oxide and alkylimdazolium salts on the thermal stability of EPDM vulcanizates. The results are given in Table 13.

The onset decomposition temperatures (T_{02}) for EPDM vulcanizates crosslinked with microsized activator was 354 °C. Applying nanosized zinc oxide alternatively to the standard activator increased the values of T_{02} and T_{05} by 9 °C and 4 °C, respectively, but had no influence on the T_{50} temperature. The use of ILs considerably increased the onset decomposition temperature of the vulcanizates and increased the T_{05} and T_{50} values by 14-17°C and 6-10°C, respectively. The increase in the thermal stability of vulcanizates resulted from the gas barrier effect of the filler network in the elastomer matrix, similar to the results obtained for the SBR elastomer. The total weight loss was approximately 75% for all examined vulcanizates.

ILs	T_{02} (°C)	T_{05} (°C)	T_{50} (°C)	Total weight loss (%)
ZnO	354	418	468	72.8
NZnO	363	422	467	75.3
DMICl	419	436	474	75.4
DIDMICl	418	436	474	75.0
DODMICl	421	437	475	75.6
HDMICl	416	437	476	75.4
MODICl	421	439	478	75.9

Table 13. Decomposition temperatures at a weight loss of 2% (T_{02}), 5% (T_{05}), 50% (T_{50}), and total weight loss during the decomposition of EPDM vulcanizates

EPDM, as previously mentioned, is widely applied in the manufacturing of rubber products for the automotive and building industries. Such rubber products are exposed to external factors such as increased temperature and UV radiation. Therefore, ILs applied as dispersing agents should not deteriorate these properties. The resistance of EPDM vulcanizates to thermo-oxidative and UV aging was studied based on the changes in the tensile parameters and crosslink densities of the vulcanizates.

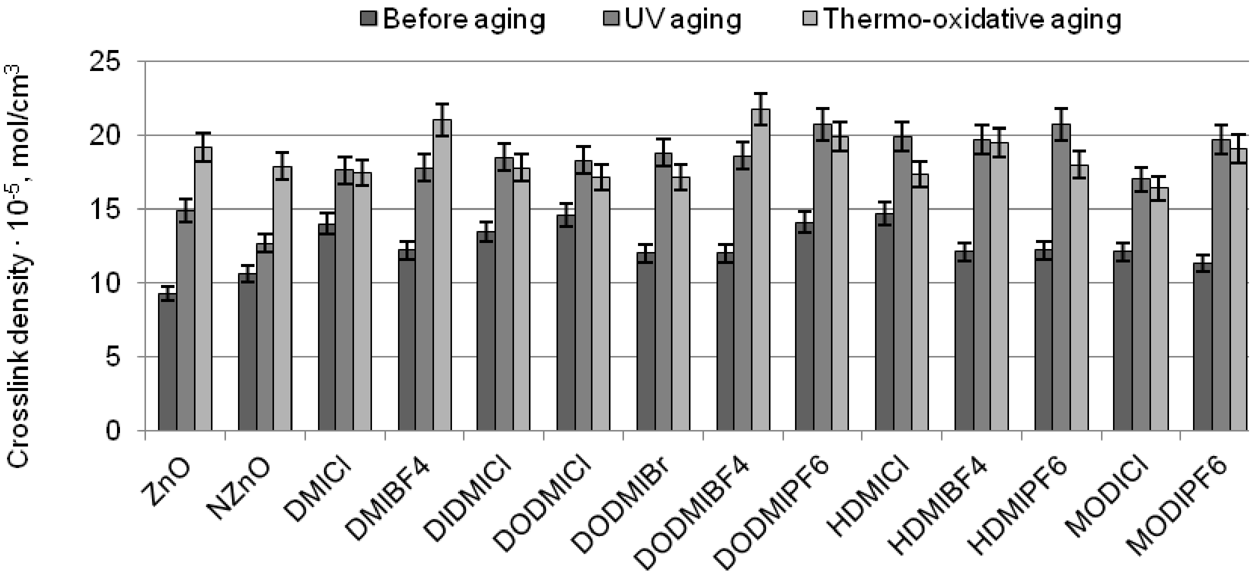

Figure 17. Crosslink density of EPDM vulcanizates after aging

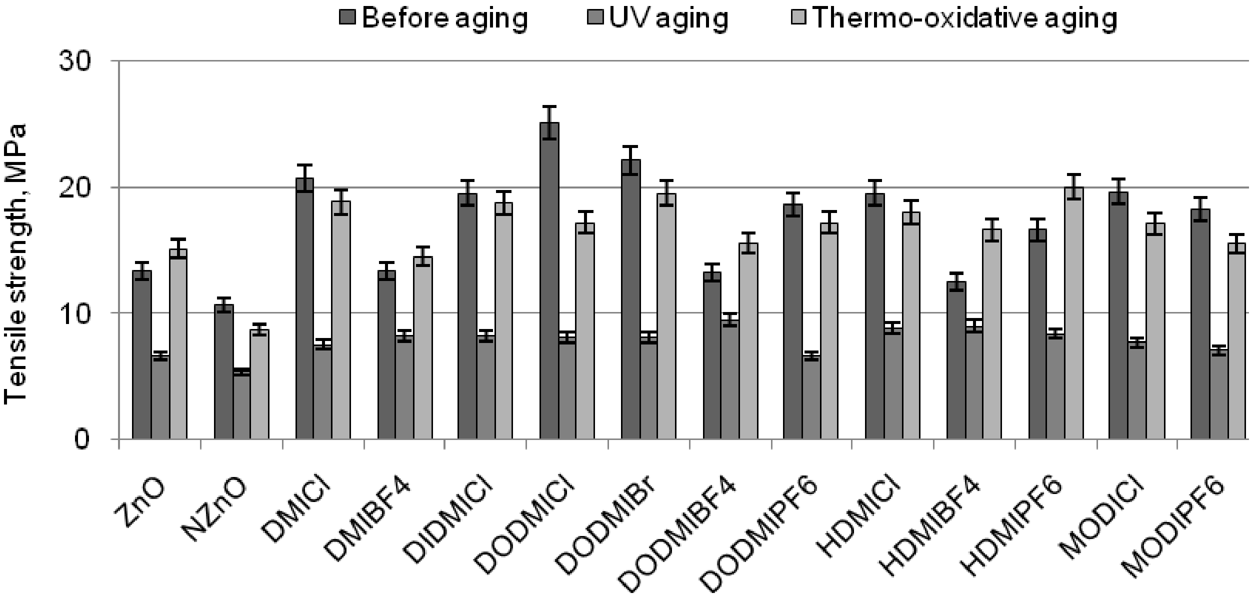

Figure 18. Tensile strength of EPDM vulcanizates after aging

Thermo-oxidative and UV aging caused the crosslink densities of the vulcanizates to increase considerably (Figure 17). It is shown that prolonged exposure to elevated temperatures and UV radiation resulted in the further crosslinking of the EPDM, similar to the case of SBR. However, the increase in the crosslink density was smaller in the case of the vulcanizates containing nanosized ZnO with DMICl, DODMICl, HDMICl, and MODICl. UV aging deteriorated the tensile strength of the vulcanizates with ILs, as the vulcanizates with nanosized ZnO (Figure 18). The highest decrease in TS was achieved for vulcanizates containing alkylimidazolium chlorides, whereas the smallest changes in TS were observed for tetrafluoroborates. Thermo-oxidative aging had less impact on the tensile strength of EPDM vulcanizates in comparison with UV radiation, and only small changes in the TS values were observed.

The aging factor was calculated to quantitatively estimate the change in the mechanical properties of the vulcanizates (Table 14). EPDM vulcanizates are highly susceptible to UV degradation. The S_{UV} values are very low (approximately 0.11). Small improvements in the S_{UV} values were achieved for vulcanizates containing alkylimidazolium tetrafluoroborates. EPDM vulcanizates exhibited higher resistance to thermo-oxidative aging, for which ILs increased the S_T values. The most active in preventing the degradation of vulcanizates upon thermo-oxidative aging were also alkylimidazolium tetrafluoroborates.

ILs	**S_{UV} (-)**	**S_T (-)**
ZnO	0.11	0.45
NZnO	0.11	0.38
DMICl	0.11	0.62
$DMIBF_4$	0.25	0.76
DIDMICl	0.12	0.67
DODMICl	0.10	0.52
DODMIBr	0.10	0.60
$DODMIBF_4$	0.32	0.79
$DODMIPF_6$	0.10	0.56
HDMICl	0.11	0.56
$HDMIBF_4$	0.25	0.90
$HDMIPF_6$	0.15	0.83
MODICl	0.10	0.53
$MODIPF_6$	0.10	0.47

Table 14. Thermo-oxidative and UV aging factors for EPDM vulcanizates

4. Conclusions

Alkylimidazolium salts considerably improved the degree of dispersion of zinc oxide and filler (silica) nanoparticles in SBR and EPDM, of which the most active seemed to be alkylimidazolium chlorides and bromide. In the IL-containing vulcanizates, nanoparticles of zinc oxide and silica were homogeneously distributed in the elastomer matrix. It can be concluded that ILs decreased the intermolecular interactions between nanoparticles and reduced their tendency for agglomeration in the elastomer.

Applying nanosized zinc oxide allowed for a reduction in the amount of ZnO by 60% in the comparison with commonly used microsized ZnO. Nanosized zinc oxide used with ILs resulted in the shortening of the optimal vulcanization time and decreased the onset vulcanization temperature by 20-30°C, which is very important from a technological and economical point of view. An increase in the crosslink density of vulcanizates was also achieved. Despite the reduced amount of zinc oxide, SBR and EPDM composites containing ILs exhibited tensile strengths higher or comparable to the standard vulcanizates crosslinked with the microsized activator. The positive effect of ILs on the vulcanization kinetics and crosslink densities of the vulcanizates results from the improvement in the degree of dispersion of ZnO nanoparticles in the elastomer. This leads to better contact between the vulcanization activator particles and other components of the crosslinking system. Of equal importance is the catalytic action of ILs in the interfacial crosslinking reactions.

Alkylimidazolium salts considerably increased the thermal stability of the vulcanizates, while ILs did not significantly increase the resistance of SBR and EPDM to UV aging. Regarding the resistance of the vulcanizates to thermo-oxidative aging, some improvement was achieved for EPDM, especially for vulcanizates containing alkylimidazolium tetrafluoroborates.

Acknowledgements

The authors wish to acknowledge the National Centre for Research and Development (Poland) for supporting this research.

Author details

Magdalena Maciejewska* and Marian Zaborski

*Address all correspondence to: magdalena.maciejewska@p.lodz.pl

Technical University of Lodz, Poland

References

[1] Sabu T, Ranimol S., editors. Rubber Nanocomposites. Preparation, Properties and Applications. Singapore: John Wiley & Sons; 2010.

[2] Wypych G., editor. Handbook of Fillers. Toronto: ChemTec Publishing; 2010.

[3] Gong H, Liu J, Baskaran S, Voise RD, Young JS. Surfactant-Assisted Processing of Carbon Nanotube/Polymer Composites. Chemistry of Materials 2000;12(4): 1049-52. http://pubs.acs.org/doi/full/10.1021/cm9906396 (accessed 17 March 2000).

[4] Dondero WE, Gorga RE. Morphological and Mechanical Properties of Carbon Nanotube/Polymer Composites via Melt Compounding. Journal of Polymer Science Part B Polymer Physics 2006;44(5): 864-78. http://onlinelibrary.wiley.com/doi/10.1002/polb.20743/pdf (accessed 25 January 2006)

[5] Ikeda Y, Poompradub S, Morita Y, Kohjiya S. Preparation of High Performance Nanocomposite Elastomer: Effect of Reaction Conditions on In Situ Silica Generation of High Content in Natural Rubber. Journal of Sol-Gel Science and Technology 2008;45(3): 299-306. http://link.springer.com/article/10.1007%2Fs10971-008-1682-7 (accessed 6 February 2008).

[6] Przybyszewska M, Krzywania A, Zaborski M, Szynkowska MI. Surface Properties of Zinc Oxide Nanoparticles Studied by Inverse Gas Chromatography. Journal of Chromatography A 2009;1216(27): 5284-91. http://www.sciencedirect.com/science/article/pii/S0021967309006827 (accessed 6 May 2009).

[7] Maciejewska M, Krzywania-Kaliszewska A, Zaborski M. Surface Properties of Calcium and Magnesium Oxide Nanopowders Grafted with Unsaturated Carboxylic Acids Studied with Inverse Gas Chromatography. Journal of Chromatography A 2012;1257(1): 141-8. http://www.sciencedirect.com/science/article/pii/S0021967312011995 (accessed 8 August 2008).

[8] Lei YD, Tang ZH, Guo BC, Zhu LX, Jia DM. Synthesis of Novel Functional Liquid and its Application as a Modifier in SBR/Silica Composites. eXPRESS Polymer Letters 2010;4(11): 692-703. http://www.expresspolymlett.com/articles/EPL-0001670_article.pdf (accessed November 2010).

[9] Subramaniam K, Das A, Heinrich G. Development of Conducting Polychloroprene Rubber Using Imidazolium Based Ionic Liquid Modified Multi-Walled Carbon Nanotubes. Composite Science and Technology 2011;71(11): 1441-9. http://www.sciencedirect.com/science/article/pii/S0266353811001928 (accessed 2 June 2011).

[10] Kreyenschulte H, Richter S, Götze T, Fischer D, Steinhauser D, Klüppel M, Heinrich G. Interaction of 1-Allyl-3-Methylimidazolium Chloride and Carbon Black and Its Influence on Carbon Black Filled Rubbers. Carbon 2012;50(10): 3649-58. http://www.sciencedirect.com/science/article/pii/S0008622312002850 (accessed 24 March 2012).

[11] Lu J, Yan F, Texter J. Advanced Applications of Ionic Liquids in Polymer Science. Progress in Polymer Science 2009; 34(5): 431-48. http://www.sciencedirect.com/science/article/pii/S0079670008001226 (accessed 13 January 2009).

[12] Rogers RD, Seddon KR. Ionic Liquids-Solvents of the Future? Science 2003;302(5646): 792-3. http://www.sciencemag.org/content/302/5646/792.full.pdf (accessed 31 October 2003).

[13] Wasserscheid P, Welton T., editor. Ionic Liquids in Synthesis. New York: Wiley-VCH; 2008.

[14] Goujon LJ, Khaldi A, Maziz A, Plesse C, Nguyen GTM, Aubert P-H, Vidal F, Chevrot C, Teyssié D. Flexible Solid Polymer Electrolytes Based on Nitrile Butadiene Rubber/Poly(ethylene oxide) Interpenetrating Polymer Networks Containing Either LiTFSI or EMITFSI. Macromolecules 2011;44(24): 9683-91. http://pubs.acs.org/doi/abs/10.1021/ma201662h (accessed 21 November 2011).

[15] Shaplov AS, Ponkratov DO, Vlasov PS, Lozinskaya EI, Malyshkina IA, Vidal F, Aubert P-H, Armand M, Vygodskii YS. Solid-State Electrolytes Based on Ionic Network Polymers. Polymer Science, Series B 2014;56(2): 164-77. http://link.springer.com/article/10.1134%2FS1560090414020134 (accessed 30 April 2014)

[16] Cho M, Seo H, Na J, Choi H, Koo J, Lee Y. High Ionic Conductivity and Mechanical Strength of Solid Polymer Electrolytes Based on NBR/Ionic Liquid and Its Application to an Electrochemical Actuator. Sensors and Actuators B 2007;128(1):70-4. http://212.51.210.219/han/ss/vls2.icm.edu.pl/pdflinks/14070321375705959.pdf (accessed 31 May 2007).

[17] Gayet F, Viau L, Leroux F, Mabille F, Monge S, Robin J-J, Voiux A. Unique Combination of Mechanical Strength, Thermal Stability and High Ion Conduction of PMMA-Silica Nanocompoistes Containing High Loadings of Ionic Liquid, Chemistry of Materials Communication 2009;21(23): 5575-7. http://pubs.acs.org/doi/abs/10.1021/cm9027918 (accessed 12 November 2009).

[18] Marwanta E, Mizumo T, Nakamura N, Ohno H. Improved Ionic Conductivity of Nitrile Rubber/Ionic Liquid Composites. Polymer 2005;46(11): 3795-800. http://212.51.210.219/han/ss/vls2.icm.edu.pl/pdflinks/14070321101005219.pdf (accessed 7 April 2005).

[19] Nockemann P, Thijs B, Pittois S, Thoen J, Glorieux C, van Hecke K, van Meervelt L, Kirchner B, Binnemans K. Task-Specific Ionic Liquid for Solubilizing Metal Oxides. Journal of Physical Chemistry B 2006;110(42): 20978-92. http://pubs.acs.org/doi/full/10.1021/jp0642995 (accessed 21 September 2006).

[20] Guo BC, Chen F, Lei YD, Liu XL, Wan JJ, Jia DM. Styrene-Butadiene Rubber/Halloysite Nanotubes Nanocomposites Modified by Sorbic Acid. Applied Surface Science 2009;255(16): 7329-36. http://www.sciencedirect.com/science/article/pii/S0169433209003663 (accessed 8 August 2008).

[21] Byrne C, McNally T. Ionic Liquid Nodification of Layered Silicates for Enhanced Thermal Stability. Macromolecular Rapid Communications 2007;28(6): 780-4. http://onlinelibrary.wiley.com/doi/10.1002/marc.200600754/full (accessed 21 March 2007).

[22] Gilman JW, Awad WH, Davis RD, Shields J, Harris RH, Davis C, Morgan AB, Sutto TE, Callahan J, Trulove H, De Long H. Polymer/Layered Silicate Nanocomposites from Thermally Stable Trialkylimidazolium-Treated Montmorillonite. Chemistry of Materials 2002;14(9): 3776-85. http://pubs.acs.org/doi/full/10.1021/cm011532x (accessed 16 August 2002).

[23] Rotkin SV, Zharov I. Nanotube Light-Controlled Electronic Switch. International Journal of Nanoscience 2002;1(3&4); 347-55. http://www.worldscientific.com/doi/pdf/10.1142/S0219581X02000280 (accessed June 2002).

[24] Bachtold A, Hadley P, Nakanishi T, Dekker C. Logic Circuits with Carbon Nanotubes Transistors. Science 2001;294(5545): 1313-7. http://www.sciencemag.org/content/294/5545/1317 (accessed 4 October 2001).

[25] Du F, Fischer JE, Winey KI. Coagulation Method for Preparing Single-Walled Carbon Nanotube/Poly(methyl methacrylate) Composites and Their Modulus, Electrical Conductivity, and Thermal Stability. Journal of Polymer Science Part B Polymer Physics 2003;41(24): 3333-8. http://onlinelibrary.wiley.com/doi/10.1002/polb.10701/full (accessed 4 November 2003).

[26] Steinhauser D, Subramanian K, Das A, Heinrich G, Klüppel M. Influence of Ionic Liquids on the Dielectric Relaxation Behavior of CNT Based Elastomer Nanocomposites. eXPRESS Polymer Letters 2012;6(11): 927-36. http://www.expresspolymlett.com/ (accessed November 2012).

[27] Das A, Stöckelhuber KW, Jurk R, Fritzsche J, Klüppel M, Heinrich G. Coupling Activity of Ionic Liquids Between Diene Elastomers and Multi-Walled Carbon Nanotubes. Carbon 2009;47(14): 3313-21. http://www.sciencedirect.com/science/article/pii/S0008622309004898 (accessed 3 August 2009).

[28] Bellayer S, Gilman JW, Eidelman N, Bourbigot S, Flambard X, Fox DM, De Long HC, Trulove PC. Preparation of Homogeneously Dispersed Multiwalled Carbon Nanotube/Polystyrene Nanocomposites via Melt Extrusion Using Trialkyl Imidazolium Compatibilizer. Advanced Functional Materials 2005;15(6): 910-6. http://onlinelibrary.wiley.com/doi/10.1002/adfm.200400441/pdf (accessed 27 May 2005).

[29] Heideman G, Noordermeer JWM, Datta RN. Effect of Zinc Complexes as Activator for Sulfur Vulcanization in Various Rubbers. Rubber Chemistry and Technology 2005;78(2): 245-57. http://rubberchemtechnol.org/doi/abs/10.5254/1.3547881 (accessed May 2005).

[30] Chapman A, Johnson T. The Role of Zinc in the Vulcanization of Styrene-Butadiene Rubbers. Kautschuk und Gummi Kunststoffe 2005;58(7-8): 358-361.

[31] Heideman G, Noordermeer JWM, Datta RN, van Baarle B. Zinc Loaded Clay as Activator in Sulfur Vulcanization: A New Route for Zinc Oxide Reduction in Rubber Compounds. Rubber Chemistry and Technology 2004;77(2): 336-55. http://www.rubberchemtechnol.org/doi/pdf/10.5254/1.3547827 (accessed May 2004).

[32] Nieuwenhuizen PJ. Zinc accelerator complexes.: Versatile homogeneous catalysts in sulfur vulcanization. Applied Catalysis A: General 2001;207(1-2): 55-68. http://www.sciencedirect.com/science/article/pii/S0926860X0000613X (accessed 8 May 2000).

[33] Przybyszewska M, Zaborski M. Effect of Ionic Liquids and Surfactants on Zinc Oxide Nanoparticle Activity in Crosslinking of Acrylonitrile Butadiene Elastomer. Journal of Applied Polymer Science, 2010;116(1): 155-64. http://onlinelibrary.wiley.com/doi/10.1002/app.31519/pdf (accessed 23 November 2009).

[34] Flory PJ, Rehner J. Statistical Mechanics of Cross-Linked Polymer Networks. II. Swelling. Journal of Chemical Physics 1943;11(11): 521-6. http://scitation.aip.org/content/aip/journal/jcp/11/11/10.1063/1.1723792 (accessed 22 December 2004).

[35] Masek A, Zaborski M, Kosmalska A. Derivatives of Flavonoides as Anti-Ageing Substances in Elastomers. Comptes Rendus Chimie 2011;14(5): 483-8. http://www.sciencedirect.com/science/article/pii/S1631074811000026 (accessed 15 February 2011).

IntechOpen